Effect of Temperature on Limit Photoconversion Efficiency in Silicon Solar Cells

Anatoly Sachenko, Vitaliy Kostylyov, Igor Sokolovskyi, and Mykhaylo Evstigneev

***Abstract*—The photoconversion efficiency and the temperature coefficient of an ideal silicon solar cell are investigated theoretically as a function of the base thickness. It is found that the efficiency depends nonmonotonically, whereas the temperature coefficient increases logarithmically with the thickness. Under the AM1.5 G illumination conditions at the temperature of 25 °C, the maximal efficiency value of 29.7% at the thickness 90 μm is obtained. The temperature coefficient has the value of 0.234%/K at the optimal base thickness. Analogous calculations were also performed for nonideal solar cells, in which the extrinsic recombination mechanisms, doping, and parasitic series and shunt resistance play a role. It is shown that all of these factors, except for the shunt resistance, result in an increase of the temperature coefficient relative to its value obtained for an ideal solar cell. In other words, the thickness-dependent value obtained for an ideal solar cell is the theoretical lower limit of the efficiency temperature coefficient if the shunting effect is negligible. The shunting resistance, in contrast, results in a further reduction of the temperature coefficient relative to the value obtained for an ideal solar cell. The implications of these findings in the solar cell design are discussed.**

***Index Terms*—Efficiency limit, silicon, solar cell (SC), temperature coefficient.**

I. Introduction

THERE exist two groups of approaches to model the photoconversion efficiency and other parameters of silicon solar cells (SCs). The first one includes various software packages, such as PC1D [1] and others [2], [3]. The other group aims at determining the limiting photoconversion efficiency in the ideal SCs. Here and in the following, the ideal SCs are those in which the extrinsic recombination mechanisms are absent, the effect of the parasitic series and shunt resistances is negligible, and optical losses do not play a role.

The research direction aiming at the estimation of the SC limiting efficiency has been initiated by the classical paper by Shockley and Queisser published in 1961 [4]. The revisions and improvements of its results have been ongoing ever since [5]–[10]. The state-of-the-art limit efficiency in silicon SCs has been established in the work [10], which improves the results of [9]. Under the AM1.5 G illumination at 25 °C, it has the value of 29.56% at the base thickness of 98.1 μm.

When calculating the limit efficiency, it is implicitly assumed that heat removal from the SC is infinitely fast, so that the SC temperature equals the environment temperature, taken to be 25 °C under the standard testing conditions. In reality, the environment temperature notably exceeds this value in places of high solar illumination. Besides, the SC temperature depends not only on the environment temperature, but also on the wind velocity, the temperature of the platform on which the SC is resting, and the heat transfer parameters between the SC and the environment. As a result, the SC inevitably heats up to the temperature that exceeds the environment temperature by tens of degrees of celsius [11]. This results in a decrease of the photoconversion efficiency that is well described by a linear empirical relation [12]–[15]

$$\eta(T) = \eta_0 \left[1 - k(T - T_0)\right] \tag{1}$$

where $T_0 = 298.15$ K is the standard reference temperature and $\eta_0 = \eta(T_0)$. This expression contains the temperature coefficient k, which has the value in the range $0.25 \ldots 0.45$%/K in silicon SCs [12]–[16]. In the literature [12]–[15], it is customary to put a plus sign in front of the $k(T - T_0)$ term of (1) and express the temperature coefficient as a negative number. We adopt an opposite sign convention, where the temperature coefficient is positive, and (1) emphasizes that $\eta(T)$ is a decreasing function of the temperature. Experimentally, the temperature coefficient is measured from two efficiency values obtained at different temperatures, $k_{\text{exp}} = (\eta(T_0) - \eta(T))/[\eta(T_0)(T - T_0)]$. The result may slightly depend on the choice of the temperature interval (T_0, T), because the curve $\eta(T)$ may slightly deviate from linearity. Therefore, in this article, the temperature coefficient is defined as a derivative as follows:

$$k = -\frac{d \ln \eta}{dT}\bigg|_{T=T_0} \tag{2}$$

and is temperature-independent.

It is obviously desirable to have the temperature coefficient as small as possible in the practical applications. The question of the smallest possible temperature coefficient clearly is both of fundamental value and practical significance, because it is directly related to the question about the highest possible photoconversion efficiency. Therefore, the performance of SCs

Manuscript received July 29, 2019; revised September 25, 2019; accepted October 20, 2019. The work of M. Evstigneev was supported by the Natural Sciences and Engineering Research Council of Canada (NSERC). *(Corresponding author: Mykhaylo Evstigneev.)*

A. Sachenko, V. Kostylyov, and I. Sokolovskyi are with the V. Lashkaryov Institute of Semiconductor Physics, National Academy of Sciences of Ukraine 03028, Kyiv, Ukraine (e-mail: sach@isp.kiev.ua; vkost@isp.kiev.ua; falcon128@gmail.com).

M. Evstigneev is with the Department of Physics and Physical Oceanography, Memorial University of Newfoundland, St. John's, NL A1B 3X7, Canada (e-mail: mevstigneev@mun.ca).

Color versions of one or more of the figures in this article are available online at http://ieeexplore.ieee.org.

Digital Object Identifier 10.1109/JPHOTOV.2019.2949418

as a function of temperature is an important research direction investigated in a number of previous publications [11]–[15].

In this article, the effect of the SC thickness, extrinsic recombination time, and the series and shunt resistance on the temperature coefficient of silicon SCs is investigated, and the lower limit of the temperature coefficient is established. Our results also suggest a somewhat more optimistic upper limit of 27.2% for silicon SC efficiency. The difference from the previously reported value of 25.6% [10] is due to two factors. First, we use an expression for the intrinsic carrier concentration from [17], whereas the calculation reported in [10] relies on an earlier expression from [18]. Second, we take into account shifting of the absorption edge to the red part of the spectrum caused by the bandgap narrowing effect, whereas this shift has been ignored in the previous analogous calculations [9], [10].

This article is organized as follows. First, we briefly outline the method for calculating the photoconversion efficiency in the ideal and nonideal SCs. This method is then applied to determine the efficiency of an ideal SC as a function of its base thickness. It is shown that the temperature coefficient increases logarithmically with the base thickness, and that the temperature coefficient value obtained for an ideal SC represents the lowest possible temperature coefficient at a given base thickness and infinite shunt resistance. The finite shunting resistance value leads to a smaller temperature coefficient value. Finally, the significance of these findings from the point of view of SC design is discussed.

II. Photoconversion Efficiency and Temperature Coefficients of a Silicon SC

A. Ideal SC

Consider first an ideal silicon SC of the $p^+ - n - n^+$ or $n^+ - p - p^+$ structure, in which the diffusion length of the minority carriers $L = \sqrt{D\tau}$ in the base is much bigger than the base thickness d. Here, D and τ are the diffusion coefficient and the effective lifetime of the minority carriers, respectively. When the condition $L \gg d$ is fulfilled, the thin-base approximation [5], [7] can be used, within which the excess carrier density Δn is uniform everywhere within the base thickness.

In an ideal SC, the net current density equals the difference between the photo-generated and recombination contributions as

$$J(V) = J_{\text{rec}}(V) - J_L. \tag{3}$$

The light-generated current density is given by

$$J_L = \frac{q}{hc}\int_0^\infty d\lambda\, \lambda\, I(\lambda)\, A_{\text{bb}}(\lambda) \tag{4}$$

where q is the elementary charge, $I(\lambda)$ is the solar spectral irradiance, and $A_{\text{bb}}(\lambda)$ is the fraction of photons whose absorption resulted in a band-to-band transition, see (18) below. The recombination current density depends on the voltage V across the base via the excess concentration Δn as

$$J_{\text{rec}}(V) = \frac{qd}{\tau}\Delta n(V). \tag{5}$$

We assume that the charge carrier concentrations in other parts of the SC are much higher than in the base. Then, the total voltage across the SC equals the voltage V across the base, and can be identified with the difference of the electron and hole quasi-Fermi levels divided by q. The product of the respective nonequilibrium concentrations in the base is related to the equilibrium electron and hole concentrations n_0 and p_0 by

$$np = (n_0 + \Delta n)(p_0 + \Delta n) = n_i^2 e^{V/V_{\text{th}}} \tag{6}$$

where n_i is the intrinsic concentration and $V_{\text{th}} = k_B T/q$ is the thermal voltage proportional to the thermal energy $k_B T$. For the excess concentration Δn, we have from the last relation

$$\Delta n(V) = -\frac{n_0 + p_0}{2} + \sqrt{\frac{(n_0 + p_0)^2}{4} + n_i^2(e^{V/V_{\text{th}}} - 1)} \tag{7}$$

where the equilibrium electron and hole concentrations are given by the expressions valid under the full dopant ionization condition

$$n_0 = \frac{n_i^2}{p_0} = \frac{N_d - N_a}{2} + \sqrt{\frac{(N_d - N_a)^2}{4} + n_i^2} \tag{8}$$

in which N_d and N_a are the donor and acceptor concentrations.

Equations (3), (5), and (7) represent the I–V curve of an ideal SC. Their use gets somewhat more complicated if one takes into account the bandgap narrowing effect by the amount ΔE_g, which depends on the carrier and doping concentrations [19]. Then, the intrinsic concentration is determined by the expression

$$n_i = n_{i0}(T) e^{\Delta E_g/(2k_B T)} \tag{9}$$

where the prefactor n_{i0} is given by [17, eq. (9)] or by [18, eq. (7)]. The bandgap narrowing ΔE_g is a rather complex function of the net electron, hole, and dopant concentration and the temperature

$$\Delta E_g = f(n_0 + \Delta n, p_0 + \Delta n, N_{\text{dop}}, T). \tag{10}$$

It is given by the sum of ion and exchange contributions for electrons and holes, see [19, eqs. (33) and (37)].

In an ideal SC only the intrinsic recombination mechanisms are present, such as radiative and Auger recombination. Then, the effective lifetime is determined by these two mechanisms as

$$\tau = \tau_{\text{intr}} = 1/(\tau_{\text{rad}}^{-1} + \tau_{\text{Auger}}^{-1}) \tag{11}$$

where the expression for the Auger lifetime is taken from [21]. For the radiative recombination lifetime, we used the expression

$$\tau_{\text{rad}}^{-1} = B_{\text{rel}}(n,p) B (1 - P_{\text{PR}})(n_0 + p_0 + \Delta n) \tag{12}$$

where B is the radiative recombination coefficient in Si [17] calculated as

$$B = \int_0^\infty dE\, B(E)$$

$$B(E) = \alpha_{\text{bb}}(E)\left(\frac{n_r(E)E}{\pi c \hbar^{3/2} n_i}\right)^2 e^{-E/(k_B T)} \tag{13}$$

the parameter $B_{\text{rel}}(n,p)$, given by [20, eq. (4)], describes the reduction of the recombination coefficient due to the screening of Coulomb attraction between electrons and holes as their concentration is increased, and P_{PR} is the photon recycling probability,

see below. Here, $n_r(E)$ and $\alpha_{\rm bb}(E)$ are the refractive index and absorption coefficient as functions of the photon energy $E = hc/\lambda$. The tables of these parameters at the temperature 300 K without band narrowing taken into account were taken from [22], and their temperature dependence was calculated according to

$$g^{\rm Green}(E,T) = g^{\rm Green}(E, 300\,{\rm K}) \left(\frac{T}{300\,{\rm K}}\right)^{b_g} \qquad (14)$$

where g refers to the parameter of interest, $g = n_r$ or $\alpha_{\rm bb}$, and the exponent b_g can be obtained from the table in [22].

In [9] and [10], the bandgap narrowing was assumed not to affect the refractive index and absorption coefficient, which were set to

$$n_r(E) = n_r^{\rm Green}(E) \quad \alpha_{\rm bb}(E) = \alpha_{\rm bb}^{\rm Green}(E). \qquad (15)$$

It can be argued, however, that the bandgap narrowing should shift the absorption edge to the red part of the spectrum by photon energy ΔE_g. Hence, the absorption coefficient should be enhanced by the bandgap narrowing. We are not aware of any publication reporting the effect of the bandgap narrowing on $\alpha_{\rm bb}$ and n_r. Therefore, as a crude approximation, we take this into account by simply shifting the photon energy by ΔE_g in the absorption coefficient, leaving the refractive index unchanged as

$$n_r(E) = n_r^{\rm Green}(E), \alpha_{\rm bb}(E) = \alpha_{\rm bb}^{\rm Green}(E + \Delta E_g). \qquad (16)$$

The photon recycling probability is given by [9]

$$P_{\rm PR} = B^{-1} \int_0^\infty dE\, A_{\rm bb}(E)\, B(E) \qquad (17)$$

where the fraction of the band-to-band transitions was found as in [10]

$$A_{\rm bb}(E) = \frac{\alpha_{\rm bb}}{\alpha_{\rm bb} + \alpha_{\rm FCA}} \frac{(1 - T_r)(1 + T_r)n_r^2}{n_r^2 - (n_r^2 - 1)T_r^2} \qquad (18)$$

where $T_r = e^{-x}(1 - x) + x^2 E_1(x)$, $x = (\alpha_{\rm bb} + \alpha_{\rm FCA})d$, and $E_1(x) = \int_x^\infty dt\, e^{-t}/t$. The second term in the denominator of the first ratio is the parasitic free-carrier absorption coefficient, found in [23].

From the maximal-power condition $d(VJ(V))/dV|_{V=V_m} = 0$, the voltage V_m is found. Substituting these into (3) allows determining the corresponding current density J_m. As a result, the photoconversion efficiency and the I–V curve fill factor are given by

$$\eta = \frac{J_m V_m}{P_S}\,,\ {\rm FF} = \frac{J_m V_m}{J_{\rm SC} V_{\rm OC}} \qquad (19)$$

where P_S is the incident irradiance, equal to 0.1 W/cm^2 under the AM1.5 G conditions, $J_{\rm SC} = J(0)$ is the short-circuit current density, and the open-circuit voltage is defined by $J(V_{\rm OC}) = 0$.

B. Nonideal SC

In a nonideal SC, extrinsic recombination mechanisms must be accounted for. To the extrinsic mechanisms belong, in particular, Shockley–Read–Hall recombination with the lifetime $\tau_{\rm SRH}$ and surface recombination with the velocity S as

$$\tau_{\rm extr} = 1/(\tau_{\rm SRH}^{-1} + S/d). \qquad (20)$$

The expression (11) for the effective lifetime is replaced with

$$\tau = 1/(\tau_{\rm intr}^{-1} + \tau_{\rm extr}^{-1}). \qquad (21)$$

In addition, including the parasitic series and shunt resistances R_S and $R_{\rm sh}$ results in a replacement of the I–V relation (3) by a more complicated expression

$$J(V) = J_{\rm rec}(V - AJR_S) + \frac{V - AJR_S}{AR_{\rm sh}} - J_L \qquad (22)$$

in which A is the SC area. At a fixed voltage V, the current density J must be determined from this equation numerically.

C. Temperature Coefficients

The expression for the temperature dependence of the SC efficiency can be expanded in a Taylor series near the reference temperature $T_0 = 298.15$ K

$$\eta(T) = \eta_0 \left[1 - k_1(T - T_0) - k_2(T - T_0)^2 - \ldots\right]. \qquad (23)$$

This expression is a generalization of (1) and can be regarded as a definition of the temperature coefficients k_i. To obtain η_0 and k_i, the efficiency η was calculated for ten temperature values from 280 to 325 K with the step size of 5 K. The so obtained support points were fitted by a third-order polynomial, and the value of k_1 found from this fit quite accurately corresponds to the derivative $d\ln\eta/dT$ at $T = T_0$. We verified that it did not change in the third significant figure as the number of support points was increased and if a higher-order fitting polynomial was used.

III. Results and Discussion

A. Validation of the Numerical Procedure

There is a certain arbitrariness in dealing with the solar irradiance data and the optical data $n_r(\lambda)$ and $\alpha_{\rm bb}(\lambda)$, which are presented in tabular form. For each wavelength interval λ_i and λ_{i+1} from the table, we approximated the corresponding dependence $g(\lambda)$ (where g represents the parameter of interest, such as I, n_r, or $\alpha_{\rm bb}$) with a cubic function using four points g_{i-1}, g_i, g_{i+1}, and g_{i+2}. This resulted in a smooth curve $g(\lambda)$. Then, all integrals were evaluated numerically using Romberg's procedure [see 24, Sec. 4.3].

In order to verify the accuracy of our code, we compare our results with those of the analogous calculations found in the literature [9], [10] for an ideal SC with $N_d = N_a = 0, \tau_{\rm extr} = \infty$, $R_S = 0$, $R_{\rm sh} = \infty$. These calculations are performed without taking into account the bandgap narrowing in $\alpha_{\rm bb}$, see (15), and with the intrinsic carrier concentration taken from [18]. When comparing our results to [9], we replaced the exact expression (18) for $A_{\rm bb}$ by the approximation used in [9], namely, $A_{\rm bb} = \alpha_{\rm bb}/[\alpha_{\rm bb} + \alpha_{\rm FCA} + (4n_r^2 d)^{-1}]$; in all other calculations reported in this article, (18) was used.

Table I compares the main photoconversion parameters with the values from [9] and [10]. It is seen that the difference between our parameters and those from [9] and [10] is the same.

TABLE I
COMPARISON OF THE EFFICIENCY AND OTHER SC PARAMETERS BETWEEN THIS ARTICLE (T.W.) AND [9], [10]

Ref.	d, μm	η, %	V_{OC}, mV	J_{SC}, mA	FF, %	V_m, mV
[9]	110	29.43	761.3	43.31	89.26	697.3
t.w.	110	29.46	759.9	43.43	89.29	696.0
[10]	98.1	29.56	763.3	43.36	89.31	699.3
t.w.	98.1	29.59	761.8	43.48	89.32	697.9

TABLE II
PHOTOCONVERSION PARAMETERS OF AN IDEAL SC OF THICKNESS $d = 98.1\ \mu$M, CALCULATED WITH (I) THE INTRINSIC CARRIER CONCENTRATION FROM [17] INSTEAD OF [18] AND (II) THE PHOTON-ENERGY SHIFTED EXPRESSION (16) FOR THE ABSORPTION COEFFICIENT INSTEAD OF ITS UNSHIFTED COUNTERPART (15)

Modification	η, %	V_{OC}, mV	J_{SC}, mA	FF, %	V_m, mV
(i)	29.65	763.3	43.48	89.32	699.3
(ii)	29.66	761.8	43.48	89.54	698.1
(i) and (ii)	29.72	763.2	43.48	89.55	699.5

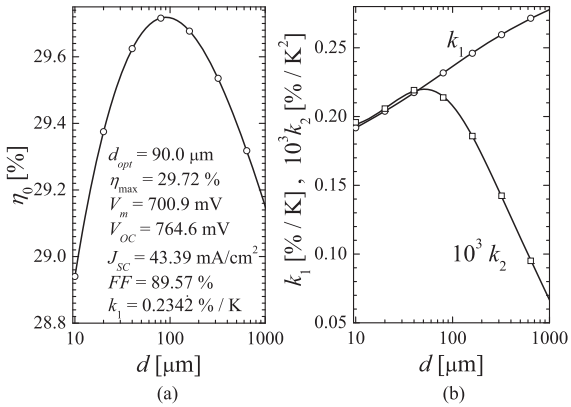

Fig. 1. (a) Efficiency at 298.15 K. (b) First two temperature coefficients of an ideal intrinsic silicon SC as a function of the base thickness. The inset in panel (a) shows the optimal thickness and the maximal efficiency, as well as the voltage at the maximal power, open-circuit voltage, short-circuit current, the fill factor, and the first temperature coefficient at $d = 90\ \mu$m. Solid lines: numerical results; symbols: polynomial approximations (24)–(26).

Our calculations yield the efficiency higher by 0.03% abs. than in [9] and [10]; our open-circuit voltage turns out to be lower than the values from [9] and [10] by 1.4 mV, etc. This difference can be attributed to the difference in the algorithms used for numerical integration. Indeed, we have found that a replacement of Romberg integration with trapezoidal integration affects the numerical values of all parameters in the fourth significant figure. For example, after integration of the expression (13), we obtained $B = 4.74 \cdot 10^{-15}$ cm^3/s, which is in agreement with the value of $4.73 \cdot 10^{-15}$ cm^3/s reported in [17]. On the other hand, in the work [9], a slightly higher value of $B = 4.82 \cdot 10^{-15}$ cm^3/s was obtained.

At the same time, the relative discrepancy between our values from Table I and the results from [9] and [10] do not exceed 0.3%. Given that the accuracy of the optical data used in the calculations ranges between 0.3% to as high as 10% [22], we consider a relative discrepancy of 0.3% between our calculations and the results from [9] and [10] as acceptable.

Coming back to the parameter values from [10], we now perform two modifications: 1) instead of the expression for the intrinsic carrier concentration from [18], we use the formula from a more recent publication [17]. Note that the empirical formula for n_{i0} in [17] is based on the data from [18] and on an additional dataset from [25]; therefore, the formula from [17] is somewhat more accurate than the one from [18]. 2) We use the photon-energy shifted expression (16) for the absorption coefficient.

The results effect of these modifications on the photoconversion parameters at $d = 98.1\ \mu$m is summarized in Table II. (i) Replacing of the intrinsic concentration expression from [18] with the one from [17] leads to an increase of the photoconversion efficiency by 0.06% abs. (ii) Shifting the argument of the absorption coefficient by the bandgap narrowing term further increases the efficiency by 0.07% abs. with the net increase being as high as 0.13% abs.

All results reported below are obtained with both modifications adopted.

B. Ideal SC

Let us consider first how the photoconversion efficiency and the first two temperature coefficients $k_{1,2}$ of an ideal SC depend on the base thickness. These curves are shown in Fig. 1. Photoconversion efficiency has a maximum at the base thickness $d = 90\ \mu$m with the corresponding limiting efficiency of 9.72%. All other parameters at the maximum are indicated in Fig. 1(a).

Near the maximum, the efficiency in Fig. 1(a) can be fitted by a cubic function of $x = \ln \frac{d}{90\ \mu\text{m}}$ as

$$\eta_0(d) = (29.718\,\%)\left(1 - 4.405 \cdot 10^{-3}x^2 + 4.623 \cdot 10^{-4}x^3\right). \tag{24}$$

With respect to the first temperature coefficient of an ideal SC, Fig. 1(b), it is a monotonically increasing function of the base thickness. It can be fitted by a third-order polynomial as

$$k_1(d) = (0.2342\,\%/\text{K})\big(1 + 8.873 \cdot 10^{-2}x - 0.6687 \cdot 10^{-3}x^2 - 1.626 \cdot 10^{-3}x^3\big). \tag{25}$$

The accuracy of the fitting expressions (24) and (25) is comparable to the line thickness in Fig. 1. At the optimal base thickness $d = 90\ \mu$m, the first temperature coefficient equals 0.234 %/K.

The second temperature coefficient is a nonmonotonic function of the base thickness, having a maximum at $d = 45\ \mu$m, where $k_2 = 2.18 \cdot 10^{-4}$ %/K^2. For the practically relevant temperatures, the magnitude of the second-order term in the expansion (23) does not exceed one-tenth of the magnitude of the first-order term. Its base thickness dependence can be approximated to a good accuracy by a fifth-order polynomial as

$$k_2(d) = (2.106 \cdot 10^{-4}\,\%/\text{K}^2)(1 - 0.1450x - 0.1130x^2 + 1.259 \cdot 10^{-2}x^3 + 8.582 \cdot 10^{-3}x^4 - 1.764 \cdot 10^{-3}x^5). \tag{26}$$

At the optimal base thickness of 90 μm, $k_2 = 2.11 \cdot 10^{-4}$ %/K^2.

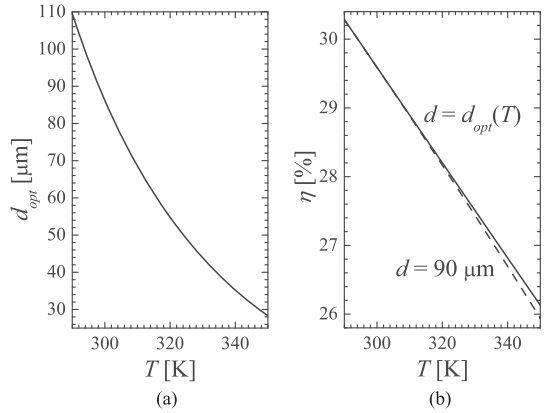

Fig. 2. (a) Optimal base thickness, at which the photoconversion efficiency of an ideal SC has a maximum, as a function of temperature. (b) Thickness-optimized efficiency (solid line) and the efficiency at the base thickness of 90 μm (dashed line) of an ideal silicon SC as a function of temperature.

These results suggest that the dependence of the temperature coefficient on thickness should be accounted for when designing a SC. In particular, the optimal thickness d_{opt} at which the photoconversion efficiency is maximized depends on the temperature and may strongly differ from the value of 90 μm obtained at $T = 25\,^{\circ}\text{C}$. This statement is illustrated for an ideal SC in Fig. 2(a), showing the optimal base thickness as a function of temperature between 290 and 350 K. In this range, the optimal thickness undergoes a fourfold decrease from 110 to 28 μm.

At the same time, the photoconversion efficiency optimized with respect to base thickness at each temperature exceeds the efficiency at a fixed thickness $d_{\text{opt}}(298.15\,\text{K}) = 90\,\mu\text{m}$ only slightly. For instance, at $T = 350$ K, the two values are 26% and 26.2%, respectively, see Fig. 2(b). This implies that from the practical point of view, working with thinner wafers may be only marginally beneficial. It should also be borne in mind that this slight efficiency enhancement may be overshadowed by the fact that thinner wafers are not as easy to handle and do not absorb light as effectively as thicker ones.

C. Nonideal SC

The expression (23) supplemented by the approximations (24)–(26) represents the highest possible efficiency of a silicon SC at a given temperature and base thickness. In view of the negative effect that all deviations from ideality have on the photoconversion efficiency, one may expect that also the temperature coefficient k_1 should increase with increasing the base doping level and the series resistance, as well as with decreasing the extrinsic lifetime and the shunt resistance. In order to verify if this is the case, let us now consider the dependence of the photoconversion efficiency and the first temperature coefficient on the doping level, extrinsic lifetime, and series resistance at infinite shunt resistance $R_{\text{sh}} = \infty$ [see Fig. 3(a)–(c)]. As seen in these figures, all these parameters indeed have a negative effect on both the efficiency and the temperature coefficient.

For instance, as seen in Fig. 3(a) and (b), an increase of the doping level results in a smaller efficiency and a larger temperature coefficient. Also note that acceptor doping is somewhat more advantageous than donor doping for both η_0 and k_1. This is due to the fact that the band-to-band Auger recombination time in p-Si is greater than in n-Si. Both curves saturate at $N_a < 10^{16}$ cm^{-3} for acceptor and at $N_d < 10^{15}$ cm^{-3} for donor doping. At the same time, there are other effects, not accounted for by our model, which lead to a higher efficiency of n-type silicon SCs. These include the formation of boron-oxygen defects, which reduce the lifetime in p-Si doped with boron [26], and a much higher sensitivity of Shockley–Read–Hall lifetime to iron concentration in p-Si than in n-Si [27]. This, in particular, explains why the SCs with the record efficiency of 26.7% [16], [28] are based on n-type silicon.

Similarly, decreasing the extrinsic lifetime results in a decrease of photoconversion efficiency and an increase in the temperature coefficient. Both characteristics saturate at $\tau_{\text{extr}} > 10$ ms. It should be noted that this criterion is not fulfilled even in the silicon SCs with the record efficiency of 26.6% reported in [28]. As estimated in [28], the extrinsic lifetime in those SCs is about 8.5 ms. In other high-efficiency SCs with $\eta < 26.6\%$, τ_{extr} has an even smaller value.

The series resistance likewise has a negative effect on both η_0 and k_1. The former characteristic decreases and the latter increases with R_S approximately linearly at $R_S < 5\,\Omega$; deviations from linearity are observed at higher R_S, but without any sign of saturation at $R_S < 10\,\Omega$.

Additional calculations have shown that simultaneous variations of several parameters τ_{extr}, N_a, N_d, and R_S at a constant R_{sh} always leads to an increase of the temperature coefficient compared to the ideal SC. Hence, the curve in Fig. 1(b) and the fitting formula (25) represent the minimal temperature coefficient at a fixed base thickness of a Si-based SC in the absence of shunting.

The photoconversion efficiency decreases as the shunt resistance is decreased, as does the temperature coefficient, see Fig. 3(d). The effect of the shunt conductance $1/R_{\text{sh}}$ on k_1 is opposite to that of a doping level, series resistance, and extrinsic lifetime. In fact, the temperature coefficient even becomes zero at $R_{\text{sh}} = 35\,\Omega$ and saturates at a negative value of -0.081%/K at $R_{\text{sh}} < 30\,\Omega$.

It should be noted that from the point of view of practical applications decreasing, the shunt resistance is not beneficial. This is so, because the decrease of the prefactor η_0 with $1/R_{\text{sh}}$ dominates, making the net efficiency $\eta_0[1 - k_1(T - T_0) - \ldots]$ a decreasing function of $1/R_{\text{sh}}$ at all temperatures.

Thus, the minimal temperature coefficient is determined by two parameters: the base thickness and the shunt resistance. To the first order in the shunt conductance $1/R_{\text{sh}}$, it can be described by

$$k_{1,\min}(d, R_{\text{sh}}) = k_1(d, \infty) - \left(\frac{y_1(d)}{AR_{\text{sh}}} + \frac{y_2(d)}{(AR_{\text{sh}})^2} + \frac{y_3(d)}{(AR_{\text{sh}})^3}\right) \quad (27)$$

where the first term is given by (25), and the functions $y_n(d)$ can be well approximated by polynomials of $x = \ln \frac{d}{90\,\mu\text{m}}$ as

$$y_n(d) = y_{n0} + y_{n1}x + y_{n2}x^2 + \cdots \quad (28)$$

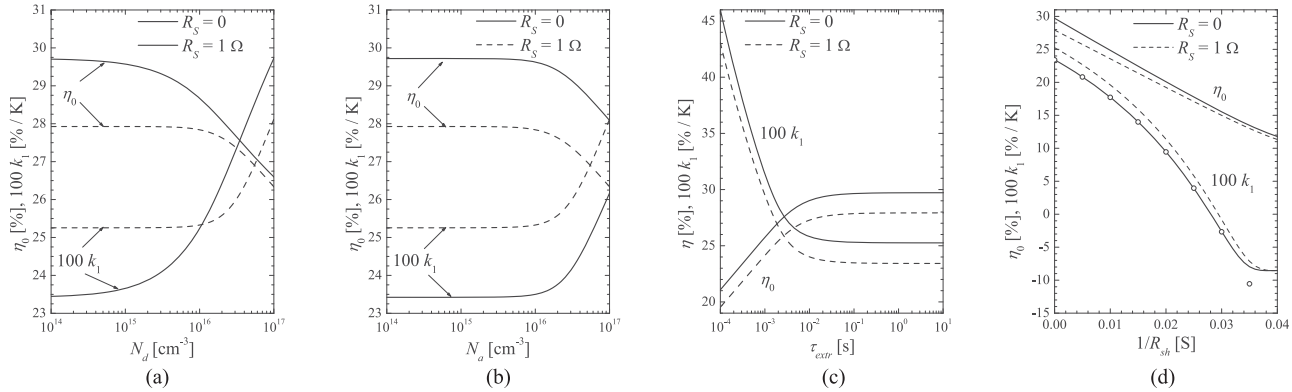

Fig. 3. Photoconversion efficiency at $T = 25\,^{\circ}$C and the first temperature coefficient of a silicon SC with the optimal base thickness $d = 90\ \mu$m and the SC area $A = 1\ \text{cm}^2$ as a function of (a) donor and (b) acceptor concentrations, (c) extrinsic lifetime, and (d) shunt resistance. The symbols in panel (d) are obtained with the approximation (27). In parts (a)–(c), the solid lines correspond to the SC with zero series resistance, and the dashed lines correspond to $R_S = 1\ \Omega$. All other parameters not explicitly mentioned in each part of the figure are set to their default ideal values, e.g., in parts (a), (b), and (d) $\tau_{\text{extr}} = \infty$; in parts (c) and (d), $N_d = N_a = 0$, etc.

TABLE III
COEFFICIENTS y_{nj} FROM (28), IN $(\Omega\,\text{CM}^2)^n$ %/K

n	y_{n0}	y_{n1}	y_{n2}	y_{n3}	y_{n4}
1	4.809	-0.1368	0.03843	0.00526	$-4.629 \cdot 10^{-4}$
2	66.73	-3.414	0.5580	0.0691	-0.0093
3	2088	-338.0	67.73	-7.372	0.3992

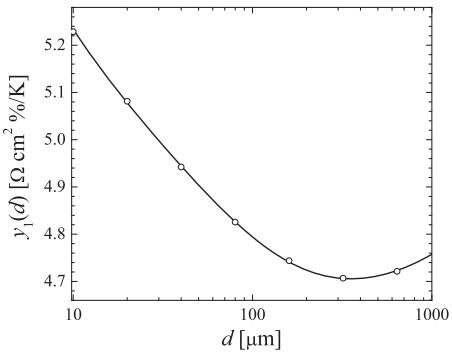

Fig. 4. Function $y_1(d)$ from (27), as obtained numerically (solid line) and with the power series (28) truncated after the third term (symbols).

The first three sets of coefficients y_{nj} for $j = 0 \ldots 4$ is presented in Table III. The approximation (28) truncated at the third term is sufficient to cover the broad range of shunt resistance values above 30 Ω, as evident from Fig. 3(d).

The typical practically relevant values of R_{sh} in silicon SCs exceed 1 kΩ; then, linear term is sufficient in the expansion (27). Presented in Fig. 4 is the corresponding coefficient $y_1(d)$ versus the base thickness as obtained numerically (solid line) and with the approximation (28) truncated at the third-order term (symbols). The agreement between the two sets of data is obvious.

Interestingly, for shunt resistance below 100 Ω, the temperature coefficient may become negative and saturate at sufficiently small R_{sh}. In that case, the photoconversion efficiency exhibits an increase with temperature above 25 °C, reach a maximum, and start decreasing. In order to describe such a temperature behavior, the linear approximation (1) is insufficient, and one needs to include the second-order temperature term, see (23).

IV. CONCLUSION

During operation, SCs inevitably heat up by tens of degrees of celsius, which results in an approximately linear decrease in the photoconversion efficiency [11]. The corresponding temperature coefficient is a fundamentally important parameter both in theory and in practical applications. If the SC efficiency depends on the base thickness nonmonotonically, developing a maximum at the optimal thickness [see Fig. 1(a) and (24)], the temperature coefficient logarithmically increases with thickness [see Fig. 1(b)]. For ideal silicon SC parameters in the thin-base approximation, it is given by the expression (25), which has a good accuracy in a broad thickness range studied. The temperature coefficient at the optimal thickness $d = 90\ \mu$m, at which the efficiency reaches the maximal value of 29.72% at 25 °C, is 0.234%/K.

The shortest lifetime related to the extrinsic recombination mechanisms, at which the efficiency of a silicon SC is not affected by recombination anymore, must be above 10 ms. From the point of view of both efficiency maximization and the minimization of the temperature coefficient, acceptor doping is more advantageous than donor doping. Both characteristics are not affected by the acceptor concentration at $N_a < 10^{16}$ cm^{-3}. At the same time, there exist other technological effects, not included into the present model, which result in a higher efficiency of the present-day n-Si SCs than p-Si ones.

Deviations of SCs from ideality result in a higher temperature coefficient at a fixed base thickness and infinite shunt resistance. Therefore, the curve in Fig. 1(b) and (25) describe the lower temperature coefficient limit at $R_{\text{sh}} = \infty$ as a function of the base thickness. At a finite shunt resistance, the temperature coefficient may become lower than the value predicted by (25), even crossing the value $k_1 = 0$ and taking on negative values at

sufficiently low R_{sh}. The smallest possible temperature coefficient is determined by the base thickness and the shunt resistance according to (27).

When designing a SC, it is desirable to maximize its efficiency by adjusting the SC thickness. Due to the base thickness dependence of the SC temperature coefficients, the optimal base thickness strongly depends on the SC operating temperature. This implies that the optimal thickness obtained under the standard testing temperature of 25 °C will not be optimal at a higher temperature. In contrast, neglecting this effect results in an ideal SC efficiency smaller by only a few tenths of a percent with respect to the optimal value.

Acknowledgments

The authors would like to thank the anonymous referees for useful suggestions. M. Evstigneev would like to thank the Atlantic Computational Excellence Network (ACENet) for computational resources and the Natural Sciences and Engineering Research Council of Canada (NSERC) for financial support.

References

[1] [Online]. Available: https://www.pveducation.org/pvcdrom/welcome-to-pvcdrom/pc1d

[2] A. Cuevas, "Modelling silicon characterisation," *Energy Procedia*, vol. 8, pp. 94–99, 2011, doi: 10.1016/j.egypro.2011.06.108.

[3] A. Fell, "A free and fast three-dimensional/two-dimensional solar cell simulator featuring conductive boundary and quasi-neutrality approximations," *IEEE Trans. Electron Devices*, vol. 60, no. 2, pp. 733–738, Feb. 2013, doi: 10.1109/TED.2012.2231415.

[4] W. Shockley and H. J. Queisser, "Detailed balance limit of efficiency of p-n junction solar cells," *J. Appl. Phys.*, vol. 32, pp. 510–519, 1961, doi: 10.1063/1.1736034.

[5] M. A. Green, "Limits on the open-circuit voltage and efficiency of silicon solar cells imposed by intrinsic Auger processes," *IEEE Trans. Electron Devices*, vol. ED-31, no. 5, pp. 671–678, May 1984, doi: 10.1109/T-ED.1984.21588.

[6] T. Tiedje, E. Yablonovitch, G. D. Cody, and B. G. Brooks, "Limiting efficiency of silicon solar cells," *IEEE Trans. Electron Devices*, vol. ED-31, no. 5, pp. 711–716, May 1984, doi: 10.1109/T-ED.1984.21594.

[7] M. A. Green, "Limiting efficiency of bulk and thin-film silicon solar cells in the presence of surface recombination," *Prog. Photovolt., Res. Appl.*, vol. 7, pp. 327–330, 1999, doi: 10.1002/(SICI)1099-159X(199907/08)7:4<327::AID-PIP250>3.0.CO;2-B.

[8] M. J. Kerr, A. Cuevas, and P. Campbell, "Limiting efficiency of crystalline silicon solar cells due to coulomb-enhanced auger recombination," *Prog. Photovolt., Res. Appl.*, vol. 11, pp. 97–104, 2003, doi: 10.1002/pip.464.

[9] A. Richter, M. Hermle, and S. W. Glunz, "Reassessment of the limiting efficiency for crystalline silicon solar cells," *IEEE J. Photovolt.*, vol. 3, no. 4, pp. 1185–1191, Oct. 2013, doi: 10.1109/JPHOTOV.2013.2270351.

[10] S. Schäfer and R. Brendel, "Accurate calculation of the absorptance enhances efficiency limit of crystalline silicon solar cells with lambertian light trapping," *IEEE J. Photovolt.*, vol. 8, no. 4, pp. 1156–1158, Jul. 2018, doi: 10.1109/JPHOTOV.2018.2824024.

[11] S. Kurtz *et al.*, "Evaluation of high-temperature exposure of photovoltaic modules," *Prog. Photovolt., Res. Appl.*, vol. 19, pp. 954–965, 2011, doi: 10.1002/pip.1103.

[12] O. Dupré, R. Vaillon, and M. A. Green, "Physics of the temperature coefficients of solar cells," *Sol. Energy Mater. Sol. Cells*, vol. 140, pp. 92–100, 2015, doi: 10.1016/j.solmat.2015.03.025.

[13] P. Singh and N. M. Ravindra, "Temperature dependence of solar cell performance—An analysis," *Sol. Energy Mater. Sol. Cells*, vol. 101, pp. 36–45, 2012, doi: 10.1016/j.solmat.2012.02.019.

[14] J. P. Seif, G. Krishnamani, B. Demaurex, C. Ballif, and S. De Wolf, "Amorphous/crystalline silicon interface passivation: Ambient-temperature dependence and implications for solar cell performance," *IEEE J. Photovolt.*, vol. 5, no. 3, pp. 718–724, May 2015, doi: 10.1109/JPHOTOV.2015.2397602.

[15] O. Dupré, R. Vaillon, and M. A. Green, "Experimental assessment of temperature coefficient theories for silicon solar cells," *IEEE J. Photovolt.*, vol. 6, no. 1, pp. 56–60, Jan. 2016, doi: 10.1109/JPHOTOV.2015.2489864.

[16] K. Yamamoto, K. Yoshikawa, H. Uzu, and D. Adachi, "High-efficiency heterojunction crystalline Si solar cells," *Jan. J. Appl. Phys.* vol. 57, pp. 08RB20:1–8, 2018, doi: 10.7567/jjap.57.08rb20.

[17] T. Trupke *et al.*, "Temperature dependence of the radiative recombination coefficient of intrinsic crystalline silicon," *J. Appl. Phys.*, vol. 94, pp. 4930–4937, 2003, doi: 10.1063/1.1610231.

[18] A. B. Sproul and M. A. Green, "Intrinsic carrier concentration and minority-carrier mobility of silicon from 77 to 300 K," *J. Appl. Phys.*, vol. 73, pp. 1214–1225, 1993, doi: 10.1063/1.353288.

[19] A. Schenk, "Finite-temperature full random-phase approximation mode of band gap narrowing for silicon device simulation," *J. Appl. Phys.*, vol. 84, pp. 3684–3695, 1998, doi: 10.1063/1.368545.

[20] P. P. Altermatt *et al.*, "Injection dependence of spontaneous radiative recombination in c-Si: Experiment, theoretical analysis, and simulation," in *Proc. 5th Int. Conf. Numer. Simul. Optoelectron. Devices*, Berlin, Germany, 2005, pp. 47–48, doi: 10.1109/NUSOD.2005.1518128.

[21] A. Richter, S. Glunz, F. Werner, J. Schmidt, and A. Cuevas, "Improved quantitative description of Auger recombination in crystalline silicon," *Phys. Rev. B*, vol. 86, 2012, Art. no. 165202, doi: 10.1103/PhysRevB.86.165202.

[22] M. A. Green, "Self-consistent optical parameters of intrinsic silicon at 300 K including temperature coefficients," *Sol. Energy Mater. Sol. Cells*, vol. 92, pp. 1305–1310, 2008, doi: 10.1016/j.solmat.2008.06.009.

[23] M. Rüdiger, J. Greulich, A. Richter, and M. Hermle, "Parameterization of free carrier absorption in highly doped silicon for solar cells," *IEEE Trans. Electron. Devices*, vol. 60, no. 7, pp. 2156–2163, Jul. 2013, doi: 10.1109/ted.2013.2262526.

[24] W. H. Press, S. A. Teukolsky, W. T. Vetterling, and B. P. Flannery, *Numerical Recipes in C*. Cambridge, U.K.: Cambridge Univ. Press, 1999.

[25] K. Misiakos and D. Tsamakis, "Accurate measurements of the silicon intrinsic carrier density from 78 to 340 K," *Appl. Phys. Lett.*, vol. 74, pp. 3293–3297, 1993, doi: 10.1063/1.354551.

[26] J. Schmidt and K. Bothe, "Structure and transformation of the metastable boron- and oxygen-related defect center in crystalline silicon," *Phys. Rev. B*, vol. 69, 2004, Art. no. 024107, doi: 10.1103/PhysRevB.69.024107.

[27] D. Macdonald and L. J. Geerligs, "Recombination activity of interstitial iron and other transition metal point defects in p- and n-type crystalline silicon," *Appl. Phys. Lett.*, vol. 85, pp. 4061–4063, 2004, doi: 10.1063/1.1812833.

[28] K. Yoshikawa *et al.*, "Exceeding conversion efficiency of 26% by heterojunction interdigitated back contact solar cell with thin film Si technology," *Sol. Energy Mater. Sol. Cell*, vol. 173, pp. 37–42, 2017, doi: 10.1016/j.solmat.2017.06.024.